Status of Muon g-2 and HVP

Lattice QCD vs. R-ratio

Kohtaroh Miura
(KEK-IPNS, Theory Center)

Talk at FPWS2022
Nov. 10, 2022

Muon Anomarous Magnetic Moment

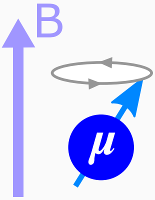

$\vec{\omega}_{spin}$

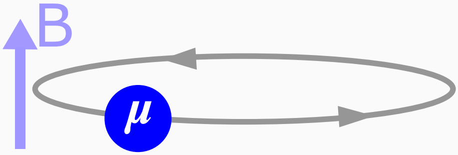

$\vec{\omega}_{cyc}$

- **Anomaly:**

$$\vec{\omega}_a = \vec{\omega}_{spin} - \vec{\omega}_{cyc} = a_\mu \frac{e\vec{B}}{m_\mu c} , \quad a_\mu = \frac{g_\mu - 2}{2} . \tag{1}$$

- **Pauli Eq.:**

$$i\hbar \frac{\partial \phi}{\partial t} = \left[\frac{(-i\hbar c\vec{\nabla} - e\vec{A})^2}{2m_\mu c} - \vec{M}_\mu \cdot \vec{B} + eA_0 \right] \phi , \quad \vec{M}_\mu = g_\mu \frac{e}{2m_\mu c} \frac{\hbar\vec{\sigma}}{2} . \tag{2}$$

Muon Anomarous Magnetic Moment in QFT

Dirac Theory

$$\vec{\omega}_a = \vec{0}\ ,\ a_\mu = 0\ ,\ g_\mu = 2\ .$$

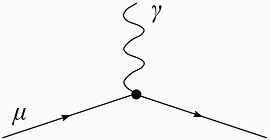

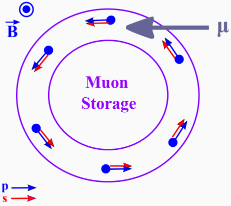

Quantum Field Theory (QFT)

$$\vec{\omega}_a \neq \vec{0}\ ,\ a_\mu > 0\ ,\ g_\mu > 2\ .$$

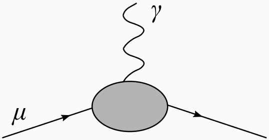

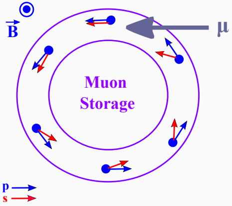

BNL-E821 / FNAL-E989

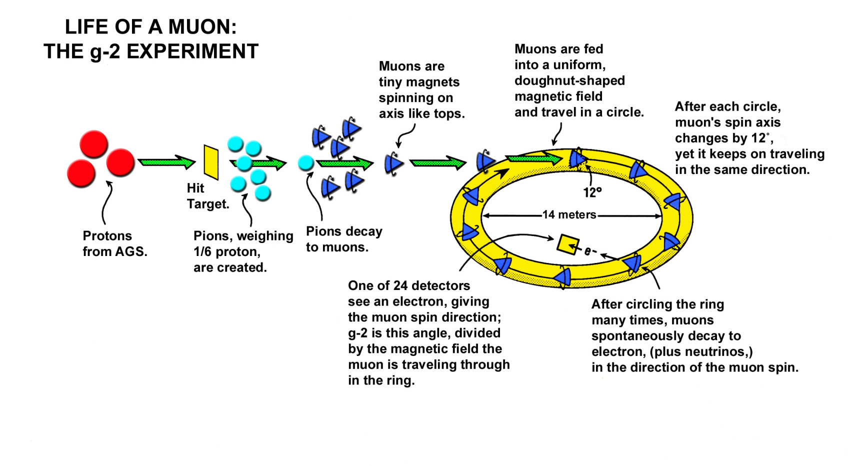

Figure: Quoted from BNL-E821 Web: https://www.g-2.bnl.gov/physics/index.html

FNAL-E989 Arrival-Time Spectrum

Model function for positron energy spectrum:

$$N_{e^+}(t, E_{th}) = N_0(E_{th}) e^{-t/(\gamma\tau_\mu)} \left(1 + A(E_{th}) \cos[\omega_a t + \phi(E_{th})]\right) . \quad (3)$$

fitted to data about $600\mu s \sim 10\gamma\tau_\mu$.

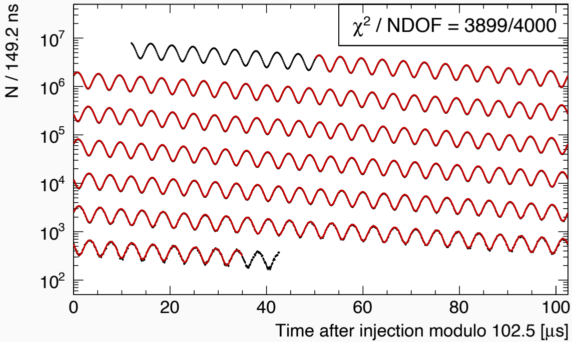

Figure: Quoted From FNAL-E989 Paper: PRD2021.

- **QFT Def. for Lepton g-2:**

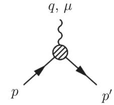

$$= \quad \langle \bar{\ell}^-(p)|\mathcal{J}^\mu|\ell^-(p')\rangle = \bar{u}(p)\Gamma^\mu(p,p')u(p')$$

$$\Gamma^\mu(q=p-p') = \gamma^\mu F_1(q^2) + \frac{i\sigma^{\mu\nu}q_\nu}{2m_\mu}F_2(q^2) + \cdots \,,$$

$$F_2(0) = a_\ell = (g_\ell - 2)/2 \,.$$

- **Standard Model, Loop Corr.:**

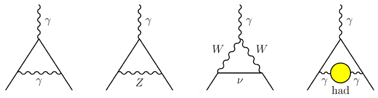

$$a_\ell^{1L\text{-QED}} = \frac{\alpha}{\pi}\int dQ^2\omega\left(\frac{Q^2}{m_\ell^2}\right) = \frac{\alpha}{2\pi}\,,$$

$$a_\ell^{\text{LO-HVP}} = \left(\frac{\alpha}{\pi}\right)^2\int dQ^2\omega\left(\frac{Q^2}{m_\ell^2}\right)\hat{\Pi}_{had}(Q^2)\,.$$

- **BSM = MSSM (Padley et.al.'15) or TC (Kurachi et.al. '13) etc.:**

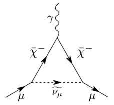

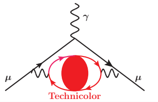

$$\propto (m_\ell/\Lambda_{BSM})^2.$$

Nobel Prize 1965

Figure: J. Schwinger, R. Feynman, S. Tomonaga. From Wikipedia.

Lamb-Shift in hydrogen atom spectra
$\rightarrow$ Quantum Vaccuum Fluctuation
$\rightarrow$ Renormalization in QED.

$$a_e = \frac{\alpha}{2\pi} \, . \tag{4}$$

Figure: Quoted from Wikipedia.

Lepton g-2: Expr. vs. SM.

- **Electron:** 2.4σ diff,
  - $a_e^{\mathrm{SM}} = 1\ 159\ 652\ 181.61(0.23) \times 10^{-12} \quad (\mathcal{O}(\alpha^5))$, with updated α [Science 360 (2018) 191 (Cs)] .
  - $a_e^{\mathrm{ex}} = 1\ 159\ 652\ 180.73(0.28) \times 10^{-12} \quad [0.24 ppb]$, [Hanneke et al '08].
- **Muon:** $a_\mu^{\mathrm{SM}} = a_\mu^{\mathrm{ex}}$?
  - $m_\mu^2/\Lambda_{BSM}^2 \sim 40000 \cdot m_e^2/\Lambda_{BSM}^2$: Much more sensitive to BSM.
  - $m_\mu \lesssim M_\pi$: Semi-stable ($\tau \sim 10^{-6}$), Non-Perturb. QCD.
- **Tau:**
  - Even more sensitive to BSM.
  - Difficult to measure due to its short life time, $\tau \sim 10^{-13}$ sec..

Lepton g-2: Expr. vs. SM.

- **Electron:** 2.4σ diff,
  - $a_e^{\mathrm{SM}} = 1\ 159\ 652\ 181.61(0.23) \times 10^{-12} \quad (\mathcal{O}(\alpha^5))$,
    with updated α [Science 360 (2018) 191 (Cs)] .
  - $a_e^{\mathrm{ex}} = 1\ 159\ 652\ 180.73(0.28) \times 10^{-12} \quad [0.24 ppb]$,
    [Hanneke et al '08].
- **Muon:** $a_\mu^{\mathrm{SM}} = a_\mu^{\mathrm{ex}}$?
  - $m_\mu^2/\Lambda_{BSM}^2 \sim 40000 \cdot m_e^2/\Lambda_{BSM}^2$: Much more sensitive to BSM.
  - $m_\mu \lesssim M_\pi$: Semi-stable ($\tau \sim 10^{-6}$), Non-Perturb. QCD.
- **Tau:**
  - Even more sensitive to BSM.
  - Difficult to measure due to its short life time, $\tau \sim 10^{-13}$ sec..

Lepton g-2: Expr. vs. SM.

- **Electron:** 2.4σ diff,
  - $a_e^{SM} = 1\ 159\ 652\ 181.61(0.23) \times 10^{-12} \quad (\mathcal{O}(\alpha^5))$, with updated α [Science 360 (2018) 191 (Cs)] .
  - $a_e^{ex} = 1\ 159\ 652\ 180.73(0.28) \times 10^{-12} \quad [0.24ppb]$, [Hanneke et al '08].
- **Muon:** $a_\mu^{SM} = a_\mu^{ex}$?
  - $m_\mu^2/\Lambda_{BSM}^2 \sim 40000 \cdot m_e^2/\Lambda_{BSM}^2$: Much more sensitive to BSM.
  - $m_\mu \lesssim M_\pi$: Semi-stable ($\tau \sim 10^{-6}$), Non-Perturb. QCD.
- **Tau:**
  - Even more sensitive to BSM.
  - Difficult to measure due to its short life time, $\tau \sim 10^{-13}$ sec..

FNAL-E989 RUN-I

2021's Biggest Breakthroughs in Physics
https://youtu.be/FMM7GWnAv0A

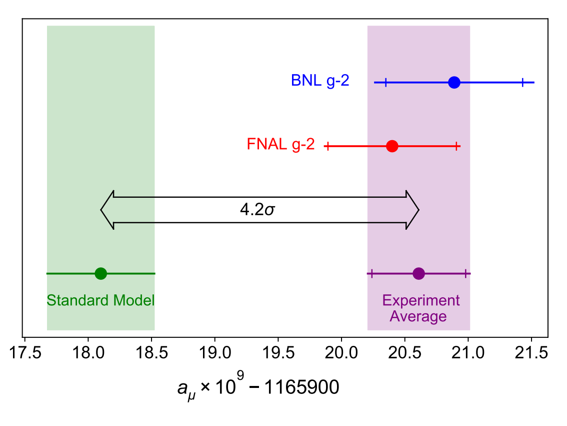

Figure: Quoted From PRL **126**, 141801 (2021)

$a_\mu^{exp.}$ vs. a_μ^{SM}

SM contribution	$a_\mu^{\rm contrib.} \times 10^{10}$	Ref.
QED [5 loops]	11658471.8931 ± 0.0104	[Aoyama et al '19]
Weak (2 loops)	15.36 ± 0.10	[Gnendiger et al '13]
LO-HVP($\mathcal{O}(\alpha^2)$) pheno.	693.1 ± 4.0	[White Paper '20]
NLO-HVP($\mathcal{O}(\alpha^3)$) pheno.	-9.84 ± 0.09	[Kurz et al '14, Jegerlehner '16]
	-9.83 ± 0.04	[KNT19]
NNLO-HVP($\mathcal{O}(\alpha^4)$) pheno.	1.24 ± 0.01	[Kurz et al '14]
HLbyL($\mathcal{O}(\alpha^3)$)	10.5 ± 2.6	[Prades et al '09]
Standard Model	11659181.0 ± 4.3 [0.37 *ppm*]	[White Paper '20]
Experiments	11659208.9 ± 6.3 [0.54 *ppm*]	[BNL-E821 '06]
	11659204.0 ± 5.4 [0.46 *ppm*]	[FNAL-E989 RUN-I '21]
	11659206.1 ± 4.1 [0.35 *ppm*]	[FNAL/BNL Combined]
Exp. $-$ SM.	25.1 ± 5.9 [4.2σ]	[FNAL/BNL - WP]

$$a_\mu^{\text{LO-HVP}}\big|_{NoNewPhys} = a_\mu^{\text{ex.}} - (a_\mu^{\text{QED}} + a_\mu^{\text{EW}} + a_\mu^{\text{(N)NLO-HVP}} + a_\mu^{\text{HLbL}}) \simeq (718.2 \pm 4.4) \times 10^{-10} \,.$$

Budget

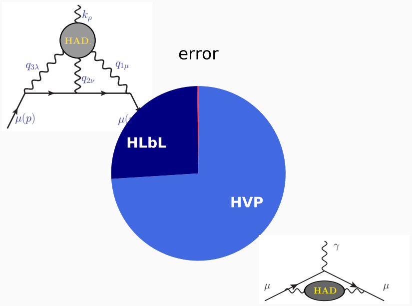

For 0.1ppm in total a_μ

- **HVP:** 0.2% precision. Challenging in LO-HVP. Tension in Pheno/LQCD?
- **HLbL:** 10% precision. Already achieved. No Tension in Pheno and LQCD.

THIS TALK

- **HVP Corrections to Running Coupling** $\hat{\Pi}(Q^2) \propto \Delta\alpha_{\rm had}(-Q^2)$

- **LO-HVP Contributions to Muon g-2** $a_\mu^{\text{LO-HVP}}$

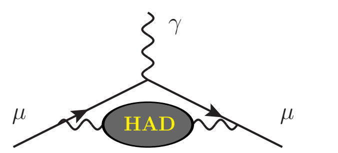

- **THIS TALK:**
  Lattice QCD vs. Data-Driven (vs. Experiments) for $\Delta\alpha_{\rm had}(-Q^2)$ and $a_\mu^{\text{LO-HVP}}$.

Table of Contents

Table of Contents

Quantum Chromo Dynamics

Quantum Chromo Dynamics (QCD)

- $SU(3)$ Gauge Theory

$$\mathcal{L} = \bar{q}\gamma^{\mu}(i\partial_{\mu} + gA^{a}_{\mu}T^{a})q - m\bar{q}q - \frac{1}{4}G^{a}_{\mu\nu}G^{\mu\nu,a}\ .$$

- Underlyning Theory of
  Quarks (q): Spin $1/2$, Fund. Rep. **3**
  Gluons (A_{μ}): Spin 1, Adjoint. Rep. **8**

- Challenging to Solve due to Non-Perturbative Property.

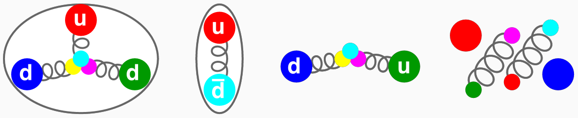

Neutron **Pion** **Diquark** **QGP**

Dispersion Relation

Unitarity:

$$F(q^2 \in \mathbb{R}) = \oint_{L+C+\bar{L}} \frac{dz}{2\pi i} \frac{F(z)}{z-q^2} \quad \text{(Cauchy)}$$

$$= \int_{L+\bar{L}} \frac{dz}{2\pi i} \frac{F(z)}{z-q^2} \qquad \text{(integrand vanish at } C\text{)}$$

$$= \int_{4M_\pi^2}^{\infty} \frac{ds}{2\pi i} \frac{F(s+i\epsilon)-F(s-i\epsilon)}{s-q^2}$$

$$= \mathcal{P}\int_{4M_\pi^2}^{\infty} \frac{ds}{2\pi i} \frac{2i\,\mathrm{Im}F(s)}{s-q^2} = \mathcal{P}\int_{4M_\pi^2}^{\infty} \frac{ds}{\pi} \frac{\mathrm{Im}F(s)}{s-q^2} \ .$$

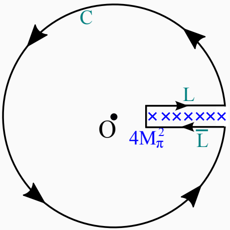

Once Subtracttion:

$$F(q^2) = \frac{\Pi(q^2)-\Pi(0)}{q^2} \Longrightarrow \hat{\Pi}(q^2) = \Pi(q^2)-\Pi(0) = q^2\,\mathcal{P}\int_{4M_\pi^2}^{\infty} \frac{ds}{\pi} \frac{\mathrm{Im}\Pi(s)}{s(s-q^2)} \ .$$

Dispersion Relation

Unitarity:

$$F(q^2 \in \mathbb{R}) = \oint_{L+C+\bar{L}} \frac{dz}{2\pi i} \frac{F(z)}{z-q^2} \quad \text{(Cauchy)}$$

$$= \int_{L+\bar{L}} \frac{dz}{2\pi i} \frac{F(z)}{z-q^2} \quad \text{(integrand vanish at } C\text{)}$$

$$= \int_{4M_\pi^2}^{\infty} \frac{ds}{2\pi i} \frac{F(s+i\epsilon)-F(s-i\epsilon)}{s-q^2}$$

$$= \mathcal{P} \int_{4M_\pi^2}^{\infty} \frac{ds}{2\pi i} \frac{2i \, \mathrm{Im} F(s)}{s-q^2} = \mathcal{P} \int_{4M_\pi^2}^{\infty} \frac{ds}{\pi} \frac{\mathrm{Im} F(s)}{s-q^2} \, .$$

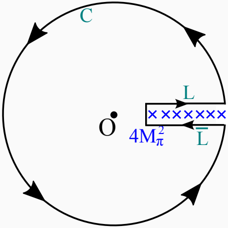

Once Subtracttion:

$$F(q^2) = \frac{\Pi(q^2)-\Pi(0)}{q^2} \Longrightarrow \hat{\Pi}(q^2) = \Pi(q^2) - \Pi(0) = q^2 \, \mathcal{P} \int_{4M_\pi^2}^{\infty} \frac{ds}{\pi} \frac{\mathrm{Im}\Pi(s)}{s(s-q^2)} \, .$$

Dispersion Relation

Unitarity:

$$F(q^2 \in \mathbb{R}) = \oint_{L+C+\bar{L}} \frac{dz}{2\pi i} \frac{F(z)}{z-q^2} \quad \text{(Cauchy)}$$

$$= \int_{L+\bar{L}} \frac{dz}{2\pi i} \frac{F(z)}{z-q^2} \quad \text{(integrand vanish at } C\text{)}$$

$$= \int_{4M_\pi^2}^{\infty} \frac{ds}{2\pi i} \frac{F(s+i\epsilon)-F(s-i\epsilon)}{s-q^2}$$

$$= \mathcal{P}\int_{4M_\pi^2}^{\infty} \frac{ds}{2\pi i} \frac{2i\,\mathrm{Im}F(s)}{s-q^2} = \mathcal{P}\int_{4M_\pi^2}^{\infty} \frac{ds}{\pi} \frac{\mathrm{Im}F(s)}{s-q^2} \,.$$

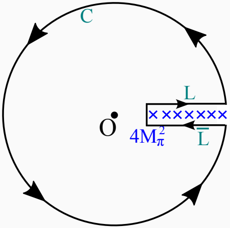

Once Subtracttion:

$$F(q^2) = \frac{\Pi(q^2)-\Pi(0)}{q^2} \Longrightarrow \hat{\Pi}(q^2) = \Pi(q^2)-\Pi(0) = q^2\,\mathcal{P}\int_{4M_\pi^2}^{\infty} \frac{ds}{\pi} \frac{\mathrm{Im}\Pi(s)}{s(s-q^2)} \,.$$

Dispersion Relation

Unitarity:

$$F(q^2 \in \mathbb{R}) = \oint_{L+C+\bar{L}} \frac{dz}{2\pi i} \frac{F(z)}{z - q^2} \quad \text{(Cauchy)}$$

$$= \int_{L+\bar{L}} \frac{dz}{2\pi i} \frac{F(z)}{z-q^2} \quad \text{(integrand vanish at } C\text{)}$$

$$= \int_{4M_\pi^2}^{\infty} \frac{ds}{2\pi i} \frac{F(s+i\epsilon)-F(s-i\epsilon)}{s-q^2}$$

$$= \mathcal{P} \int_{4M_\pi^2}^{\infty} \frac{ds}{2\pi i} \frac{2i\ \mathrm{Im}F(s)}{s-q^2} = \mathcal{P} \int_{4M_\pi^2}^{\infty} \frac{ds}{\pi} \frac{\mathrm{Im}F(s)}{s-q^2} \ .$$

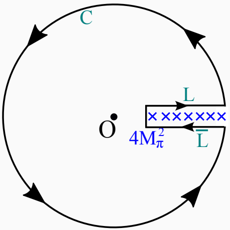

Once Subtracttion:

$$F(q^2) = \frac{\Pi(q^2) - \Pi(0)}{q^2} \Longrightarrow \hat{\Pi}(q^2) = \Pi(q^2) - \Pi(0) = q^2\ \mathcal{P} \int_{4M_\pi^2}^{\infty} \frac{ds}{\pi} \frac{\mathrm{Im}\Pi(s)}{s(s-q^2)} \ .$$

Dispersion Relation

Unitarity:

$$F(q^2 \in \mathbb{R}) = \oint_{L+C+\bar{L}} \frac{dz}{2\pi i} \frac{F(z)}{z-q^2} \quad \text{(Cauchy)}$$

$$= \int_{L+\bar{L}} \frac{dz}{2\pi i} \frac{F(z)}{z-q^2} \quad \text{(integrand vanish at } C\text{)}$$

$$= \int_{4M_\pi^2}^{\infty} \frac{ds}{2\pi i} \frac{F(s+i\epsilon)-F(s-i\epsilon)}{s-q^2}$$

$$= \mathcal{P} \int_{4M_\pi^2}^{\infty} \frac{ds}{2\pi i} \frac{2i\, \mathrm{Im}F(s)}{s-q^2} = \mathcal{P} \int_{4M_\pi^2}^{\infty} \frac{ds}{\pi} \frac{\mathrm{Im}F(s)}{s-q^2} \, .$$

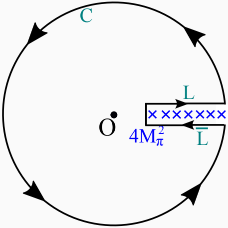

Once Subtracttion:

$$F(q^2) = \frac{\Pi(q^2)-\Pi(0)}{q^2} \Longrightarrow \hat{\Pi}(q^2) = \Pi(q^2) - \Pi(0) = q^2\, \mathcal{P} \int_{4M_\pi^2}^{\infty} \frac{ds}{\pi} \frac{\mathrm{Im}\Pi(s)}{s(s-q^2)} \, .$$

HVP Phenomenology

- HVP in Pheno:

$$\hat{\Pi}(-Q^2) = \int_0^\infty ds \frac{Q^2}{s(s+Q^2)} \frac{\mathrm{Im}\Pi(s)}{\pi} \quad \text{(dispersion)} ,$$

$$= \frac{Q^2}{12\pi^2} \int_0^\infty ds \frac{R(s)}{s(s+Q^2)} \quad \text{(optical)} .$$

- R-ratio:

$$R(s) \equiv \frac{\sigma(e^+e^- \to \gamma^* \to had.)}{4\pi\alpha^2(s)/(3s)} .$$

- Systematics is challenging to control. Some tension among experiments in $\sigma(e^+e^- \to \pi^+\pi^-)$.

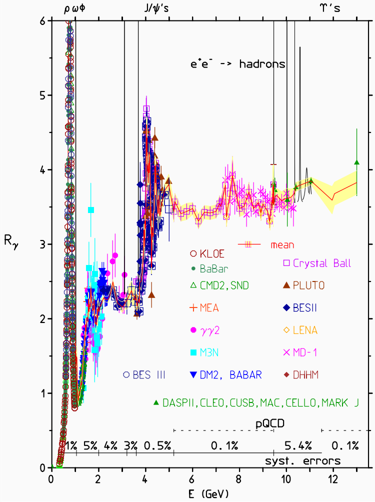

[Jegerlehner EPJ-Web2016]

HVP Phenomenology

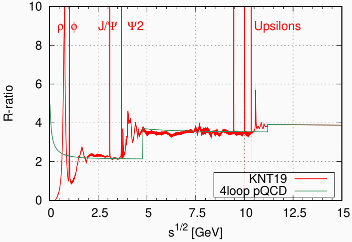

- HVP in Pheno:

$$\hat{\Pi}(-Q^2) = \int_0^\infty ds \frac{Q^2}{s(s+Q^2)} \frac{\mathrm{Im}\Pi(s)}{\pi} \quad \text{(dispersion)} \,,$$

$$= \frac{Q^2}{12\pi^2} \int_0^\infty ds \frac{R(s)}{s(s+Q^2)} \quad \text{(optical)} \,.$$

- R-ratio:

$$R(s) \equiv \frac{\sigma(e^+e^- \to \gamma^* \to had.)}{4\pi\alpha^2(s)/(3s)} \,.$$

- Systematics is challenging to control. Some tension among experiments in $\sigma(e^+e^- \to \pi^+\pi^-)$.

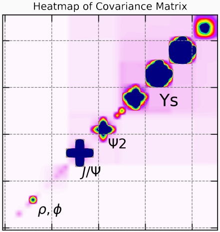

Figs: KNT Data in PRD2018. Thanks to Alex Keshavarzi.

Data-Driven HVP

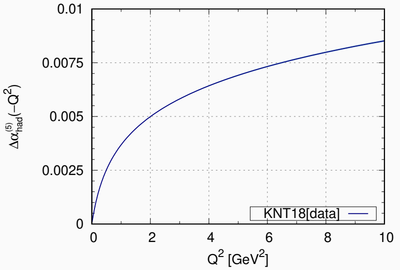

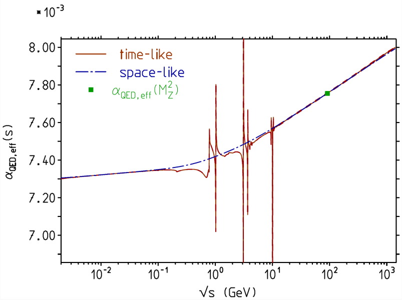

Fig: Five-flavor QCD/Hadronic contribution to QED running coupling,

$$\Delta\alpha^{(5)}_{\rm had}(s) = 4\pi\alpha_0 \hat{\Pi}^{u,d,s,c,b}(s)\ , \quad \alpha_0 = \frac{1}{137.03...}\ . \tag{5}$$

The spacelike case (left, KNT-2018 data) and the timelike one (right, Jegerlehner alphaQEDc19 manual).

Table of Contents

Lattice Gauge Theory

- Action: $S_{LQCD} = S_G[U, a] - \bar{\psi}\, D[U, m, a]\, \psi$.
  $\xrightarrow{a \to 0} S_{QCDcnt.}$
- S_{LQCD} respects Exact Gauge Symmetry.
- Observable:
  $\langle O \rangle = \int_U P[U] O[U]$, $\quad P = e^{-S_G}\,\mathrm{Det}[D]/Z$.
- Hybrid Monte Carlo: $\{U^{(i)}\}$ created w. P.

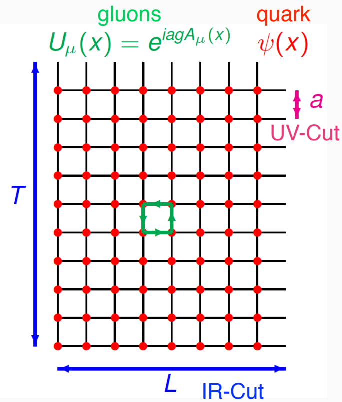

Lattice Gauge Theory

LQCD Inputs

- Lattice Coupling: $\beta(a) = 2N_c/g^2(a)$.
- Fermion Masses: $m_{ud},\ m_s,\ m_c$.
- (Isospin Breaking): $\alpha_0 = \frac{1}{137.03\cdots},\ \frac{m_u}{m_d} = 0.485$.

LQCD Outputs

- Hadron Masses: $M_{\pi,K,\dots}/M_\Omega,\quad F_\pi/M_\Omega$, etc.
- Vector Current Corr.: $\langle(\bar\psi\gamma_\mu\psi)_x(\bar\psi\gamma_\nu\psi)\rangle_{y=0}$.

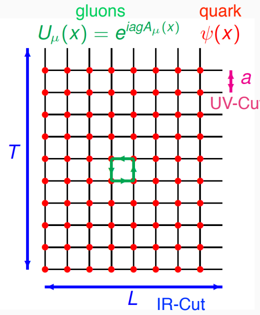

Lattice Gauge Theory V

LQCD: Non-Perturb. Def. of QCD

- Latticize w. $a \Leftrightarrow$ Dimentional regularization etc.
- Continuum limit ($a \to 0$) $\Leftrightarrow$ Renormalization.
- A line of constant physics: $a \to 0$ with $m_{u,d,s,c}$ adjusted to keep $M_{\pi,K,\cdots}/M_{\Omega}$ e.t.c.
- First-Principle Cal. (no free param.)
- Stringent Algorithm (no approx. in HMC.)

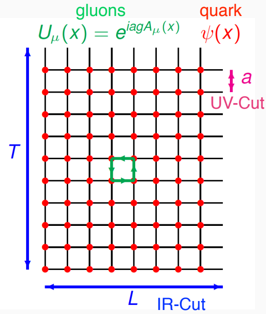

Lattice QCD Gluon Action

- **Plaquette**

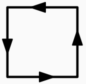

$$U_{\nu\rho,x} \sim e^{ia^2 g\ G_{\nu\rho,x}}$$

- **Action for Gluons**

$$S_G = \sum_{\nu\rho,x} \frac{2N_c}{g^2}\left[1 - \frac{\mathrm{tr}_c}{2N_c}\left[U_{\nu\rho,x} + U^{\dagger}_{\nu\rho,x}\right]\right] \xrightarrow{a\to 0} \frac{1}{4}\int d^4x\ G_{\nu\rho,x}G^{\nu\rho}_x \tag{6}$$

- **Strong Coupling ($1/g^2$) Expansion**

$$Z = \int DU\ e^{-S_G[U]} = \int DU\left(1 - S_G[U] + \frac{1}{2}S_G^2[U] + \cdots\right). \tag{7}$$

- **Haar Measure Integral (finite examples)**

$$\int dU = \mathbf{1}\,, \quad \int dU\ U_a^{\bar{a}} U_b^{\dagger\bar{b}} = \frac{\delta_a^{\bar{b}}\delta_b^{\bar{a}}}{N_c}\,, \quad \int dU\ U_a^{\bar{a}} U_b^{\bar{b}} U_c^{\bar{c}} = \frac{\epsilon_{abc}\ \epsilon^{\bar{a}\bar{b}\bar{c}}}{N_c!}\,. \tag{8}$$

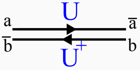

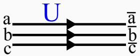

Wilson Loop at Strong Coupling Limit

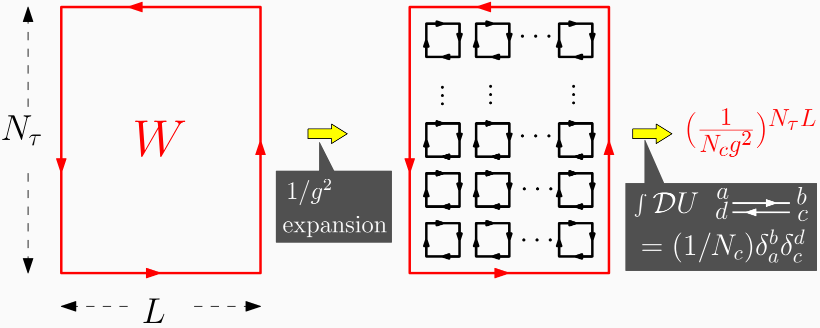

Gluons $\sim$ Plaquette $\sim$ Area Law

$$\langle W[U] \rangle = \frac{1}{Z} \int DU \, e^{-S_G[\Box_U]} W[U] = N_c e^{-N_\tau V_{pot}(L)} , \tag{9}$$

$$V_{pot}(L) = L \times \kappa , \qquad \kappa = \frac{1}{a^2} \log[g^2 N_c] \quad \text{(String Tension)} . \tag{10}$$

LQCD Monte Carlo

It is hopeless to count analytically all possible plaquette tiling (and quark hoppings). We need Monte Carlo simulations.

1. Give $U_{i=\text{label of step}}$. At 1st, unit $\mathbf{1}$ or $SU(3)$ random matrices.
2. Calculate $P_i = \mathrm{Det} D[U_i]\, e^{-S_G[U_i]}$.
3. Generate U_{i+1} w probability weight P_i.
   - Heat-Bath (HB) Method: local action. e.g. pure Yang-Mills $S_G \propto \sum_{\nu,x} \mathrm{Tr}_c U_{\nu,x} V_{\nu,x}$.
   - Hybrid Monte Carlo (HMC) Method: Molecular Dynamics (EoM) + Metropolis (Accept/Reject). Non-local action. e.g. with quark hopping $\mathrm{Det} D[U]$.
4. With updated U_{i+1}, go back to the first step. Repeat till an observable $O[U_i]$ gets stable (thermalization).

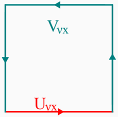

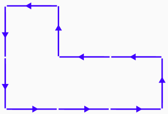

LQCD Meas. of HVP and $a_\mu^{\text{LO-HVP}}$

$\{U^{(i)}\}$: HMC

$\downarrow$

$D_f[U] \equiv D[U, m_f]$: Dirac Op.

$\downarrow$ Solve Dirac Eq.

$D_f^{-1}[U]$: Quark Propagator.

$\downarrow$

Vector Current Correlator

$$G^f_{\mu\nu}(x) = \langle (\bar\psi\gamma_\mu\psi)_x(\bar\psi\gamma_\nu\psi)_{y=0}\rangle \xrightarrow[\text{wick}]{}$$

$$C^f_{\mu\nu}(x) = -\langle \mathrm{ReTr}[\gamma_\mu D^{-1}_{f,x0}\gamma_\nu D^{-1}_{f,0x}]\rangle ,$$

$$D^f_{\mu\nu}(x) = \langle \mathrm{Re}[\mathrm{Tr}[\gamma_\mu D^{-1}_{f,xx}]\mathrm{Tr}[\gamma_\nu D^{-1}_{f,yy}]_{y=0}]\rangle ,$$

$\downarrow$

HVP: $\Pi^f_{\mu\nu}(Q) = \mathcal{F}.\mathcal{T}.[G^f_{\mu\nu}(x)]$,

g-2: $a^{\text{LO-HVP}}_{\mu,f} = (\frac{\alpha}{\pi})^2 \sum_t W(t, m_\mu^2) G^f(t)$.

BMW2020 finest lattice ensembles.

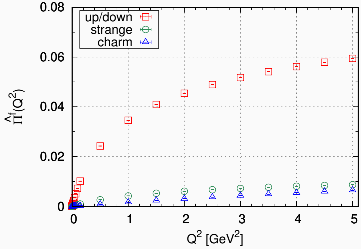

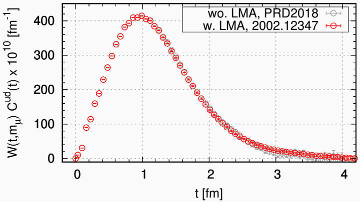

LQCD Meas. of HVP and $a_\mu^{\text{LO-HVP}}$

$\{U^{(i)}\}$: HMC

$\downarrow$

$D_f[U] \equiv D[U, m_f]$: Dirac Op.

$\downarrow$ Solve Dirac Eq.

$D_f^{-1}[U]$: Quark Propagator.

$\downarrow$

Vector Current Correlator

$$G^f_{\mu\nu}(x) = \langle (\bar\psi\gamma_\mu\psi)_x(\bar\psi\gamma_\nu\psi)_{y=0}\rangle \xrightarrow[\text{wick}]{}$$

$$C^f_{\mu\nu}(x) = -\langle \mathrm{ReTr}[\gamma_\mu D^{-1}_{f,x0}\gamma_\nu D^{-1}_{f,0x}]\rangle ,$$

$$D^f_{\mu\nu}(x) = \langle \mathrm{Re}\left[\mathrm{Tr}[\gamma_\mu D^{-1}_{f,xx}]\mathrm{Tr}[\gamma_\nu D^{-1}_{f,yy}]_{y=0}\right]\rangle ,$$

$\downarrow$

HVP: $\Pi^f_{\mu\nu}(Q) = \mathcal{F.T.}[G^f_{\mu\nu}(x)]$,

g-2: $a^{\text{LO-HVP}}_{\mu,f} = (\frac{\alpha}{\pi})^2 \sum_t W(t, m_\mu^2) G^f(t)$.

BMW2020 finest lattice ensembles.

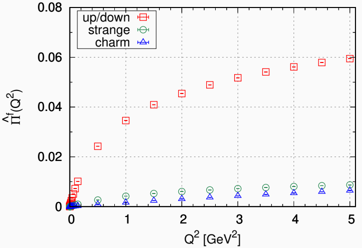

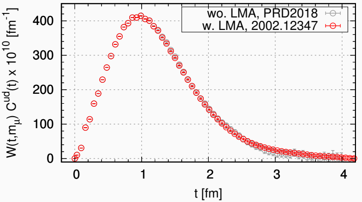

LQCD Meas. of HVP and $a_\mu^{\text{LO-HVP}}$

$\{U^{(i)}\}$: HMC

$\downarrow$

$D_f[U] \equiv D[U, m_f]$: Dirac Op.

$\downarrow$ Solve Dirac Eq.

$D_f^{-1}[U]$: Quark Propagator.

$\downarrow$

Vector Current Correlator

$$G^f_{\mu\nu}(x) = \langle (\bar\psi\gamma_\mu\psi)_x(\bar\psi\gamma_\nu\psi)_{y=0}\rangle \xrightarrow[\text{wick}]{}$$

$$C^f_{\mu\nu}(x) = -\langle \mathrm{ReTr}[\gamma_\mu D^{-1}_{f,x0}\gamma_\nu D^{-1}_{f,0x}]\rangle\ ,$$

$$D^f_{\mu\nu}(x) = \langle \mathrm{Re}\left[\mathrm{Tr}[\gamma_\mu D^{-1}_{f,xx}]\mathrm{Tr}[\gamma_\nu D^{-1}_{f,yy}]_{y=0}\right]\rangle\ ,$$

$\downarrow$

HVP: $\Pi^f_{\mu\nu}(Q) = \mathcal{F.T.}[G^f_{\mu\nu}(x)]\ ,$

g-2: $a^{\text{LO-HVP}}_{\mu,f} = (\frac{\alpha}{\pi})^2\sum_t W(t, m_\mu^2)G^f(t)\ .$

BMW2020 finest lattice ensembles.

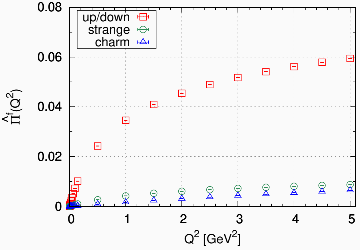

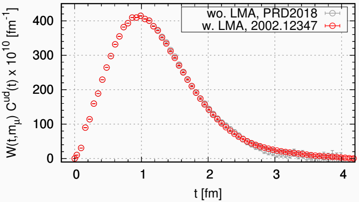

Table of Contents

Mainz HVP Working Group

M. Cè, A. Géradin, G. Hippel, R. Hudspith, S. Kuberski, H.B. Meyer, K. Miura, D. Mohler, K. Ottnad, S. Paul, A. Risch, T. San José, J. Wilhelm, and H. Wittig.

JHEP2022 and arXiv:2206.06582 [hep-lat]

Comparison of $\Delta\alpha^{(5)}_{\rm had}(-Q^2)$

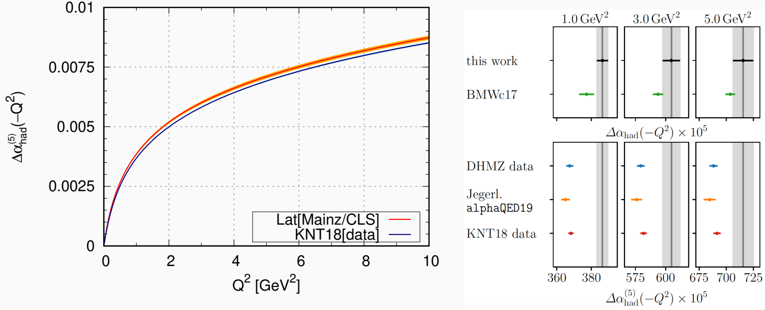

- **Fig.** Left: LQCD [Mainz-JHEP22] vs. Pheno(KNT18[data], [KNT-PRD18]) for $\Delta\alpha^{(5)}_{\rm had}(-Q_0^2) \propto \hat{\Pi}^{u,d,s,c,b}(-Q^2)$. Right: Detailed comparisons.
- Mainz results are consistent with BMWc17 but larger than phenomenological estimates with a few sigma tension.
- Larger $\Delta\alpha^{(5)}_{\rm had}(-Q_0^2) \iff$ larger $a_\mu^{\text{LO-HVP}}$.

$\Delta\alpha^{(5)}_{\rm had}(-Q^2)$ Summary

Error Type	%	Comments
statistical	1.1	simulation based
chiral/continuum extrap.	0.1	simulation based
scale setting	0.7	simulation based
isospion breaking	0.3	simulation based
charm sea-quark	0.3	D-meson pheno.
charm disconnected	~ 0.01	1% of uds-disc. c.f. [BMW-PRL18]
bottom	0.3	w. time-moments by [HPQCD-PRD2015]

Table: Error Budget in $\Delta\alpha^{(5)}_{\rm had}(-5GeV^2) = 0.00716(8)_{sta}(0)_{fit}(5)_{scale}(2)_{isb}(2)_{c\text{-}sea}(2)_b$[9].

- $\Delta\alpha^{(5)}_{\rm had}(-Q_0^2)|_{\rm central} = \Delta\alpha^{\rm Mainz}_{\rm had}(-Q_0^2)|_{\rm central}$ from $N_f = 2+1$ ensembles.
- Isospin breaking, charm-sea/disc, and bottom effects are considered into systematic errors.

Euclidean Split Method

- Euclidean Split Method:

$$\Delta\alpha^{(5)}_{\rm had}(M_Z^2) = \Delta\alpha^{(5)}_{\rm had}(-Q_0^2) \longleftarrow \text{LQCD / R-ratio}$$

$$+\left[\Delta\alpha^{(5)}_{\rm had}(-M_Z^2) - \Delta\alpha^{(5)}_{\rm had}(-Q_0^2)\right] \longleftarrow \text{pQCD}'$$

$$+\left[\Delta\alpha^{(5)}_{\rm had}(M_Z^2) - \Delta\alpha^{(5)}_{\rm had}(-M_Z^2)\right] \longleftarrow 0.000045(\text{pQCD}) \,.$$

- c.f. Usual R-ratio Method (Data-Driven Pheno.):

$$\Delta\alpha^{(5)}_{\rm had}(M_Z^2) = -\frac{\alpha_0 M_Z^2}{3\pi}\,\mathcal{P}\int_{4M_\pi^2}^{\infty} ds\,\frac{R(s)}{s(s-M_Z^2)}\,.$$

pQCD′[Adler]

- Naive expression for higher energy corrections:

$$\left[\Delta\alpha_{\rm had}^{(5)}(-M_Z^2)-\Delta\alpha_{\rm had}^{(5)}(-Q_0^2)\right]=\frac{\alpha_0}{3\pi}(M_Z^2-Q_0^2)\int_{m_{\pi^0}^2}^{\infty}ds\,\frac{R(s)}{(s+Q_0^2)(s+M_Z^2)}\,.$$

- Higher energy corrections w.r.t. Adler function $D(-Q^2)$:

$$\left[\Delta\alpha_{\rm had}^{(5)}(-M_Z^2)-\Delta\alpha_{\rm had}^{(5)}(-Q_0^2)\right]=\frac{\alpha_0}{3\pi}\int_{Q_0^2}^{M_Z^2}\frac{dQ^2}{Q^2}D(-Q^2)\,,\qquad(11)$$

where $D(-Q^2)=(3\pi/\alpha_0)[s\,d\Delta\alpha_{\rm had}^{(5)}(s)/ds]_{s=-Q^2}$.

- For the Adler function, pQCD relatively works:

  pQCD′[Adler] = pQCD + Operator Product Expn. + Padè fits

  captures J/Ψ and Υ resonances.

pQCD′[Adler]

- Naive expression for higher energy corrections:

$$\left[\Delta\alpha^{(5)}_{\rm had}(-M_Z^2) - \Delta\alpha^{(5)}_{\rm had}(-Q_0^2)\right] = \frac{\alpha_0}{3\pi}(M_Z^2 - Q_0^2)\int_{m^2_{\pi^0}}^{\infty} ds \frac{R(s)}{(s+Q_0^2)(s+M_Z^2)} \,.$$

- Higher energy corrections w.r.t. Adler function $D(-Q^2)$:

$$\left[\Delta\alpha^{(5)}_{\rm had}(-M_Z^2) - \Delta\alpha^{(5)}_{\rm had}(-Q_0^2)\right] = \frac{\alpha_0}{3\pi}\int_{Q_0^2}^{M_Z^2} \frac{dQ^2}{Q^2} D(-Q^2) \,, \qquad (11)$$

where $D(-Q^2) = (3\pi/\alpha_0)[s\, d\Delta\alpha^{(5)}_{\rm had}(s)/ds]_{s=-Q^2}$.

- For the Adler function, pQCD relatively works:

  pQCD′[Adler] = pQCD + Operator Product Expn. + Padè fits

  captures J/Ψ and Υ resonances.

Adler Function

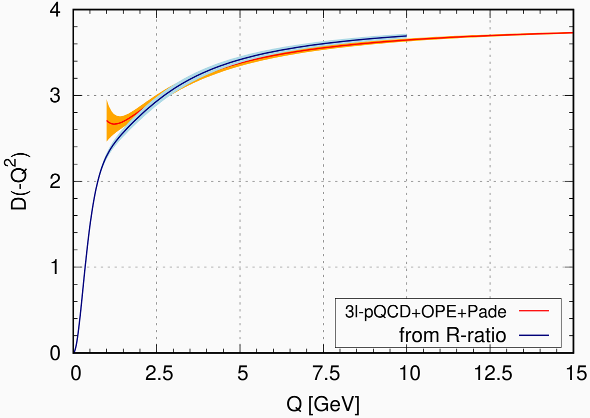

Red: $D(-Q^2)$ using pQCD′ = 3l-pQCD + OPE + Padè.

Blue: $D(-Q^2) = Q^2 \int_{4M_\pi^2}^{\infty} ds\, R(s)/(s+Q^2)^2$.

Euclidean Split Method

- Euclidean Split Method:

$$\Delta\alpha^{(5)}_{\rm had}(M_Z^2) = \Delta\alpha^{(5)}_{\rm had}(-Q_0^2) \longleftarrow \text{LQCD / R-ratio}$$

$$+\left[\Delta\alpha^{(5)}_{\rm had}(-M_Z^2) - \Delta\alpha^{(5)}_{\rm had}(-Q_0^2)\right] \longleftarrow \text{pQCD}'$$

$$+\left[\Delta\alpha^{(5)}_{\rm had}(M_Z^2) - \Delta\alpha^{(5)}_{\rm had}(-M_Z^2)\right] \longleftarrow 0.000045(\text{pQCD}) \,.$$

- c.f. Usual R-ratio Method (Data-Driven Pheno.):

$$\Delta\alpha^{(5)}_{\rm had}(M_Z^2) = -\frac{\alpha_0 M_Z^2}{3\pi}\,\mathcal{P}\int_{4M_\pi^2}^{\infty} ds\,\frac{R(s)}{s(s-M_Z^2)} \,.$$

QED Coupling at Z-pole with Mainz LQCD

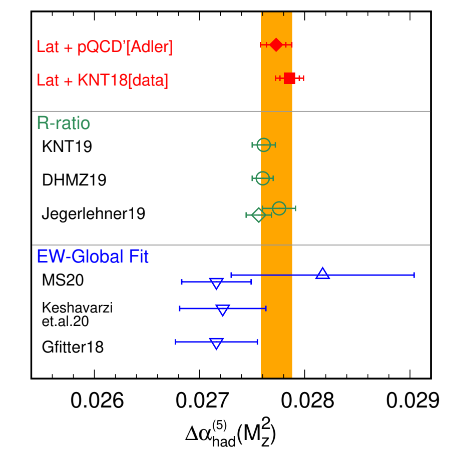

Figure: 5-flavor quark/hadron contributions to QED coupling at Z-pole.

Mainz LQCD, JHEP-2022

- ♦ = Mainz LQCD + pQCD′[Adler]: $\Delta\alpha^{(5)}_{\rm had}(M_Z^2) = 0.02773(9)_{\rm lat}(2)_{\rm heavy}(12)_{\rm pQCD'[Adler]}[15]_{\rm tot}$.
- ■ = Mainz LQCD + KNT18[data] = consistent to ♦.

QED Coupling at Z-pole Comparison I

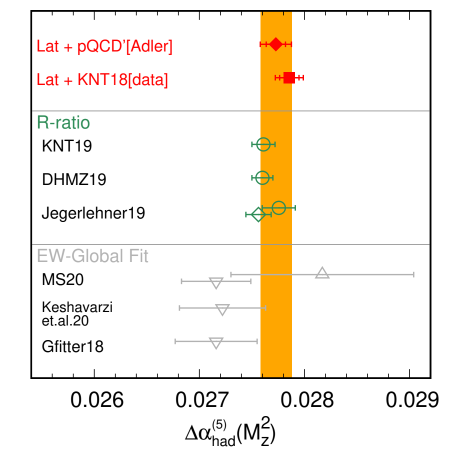

Figure: 5-flavor quark/hadron contributions to QED coupling at Z-pole.

Mainz LQCD, JHEP-2022

- First symbol ♦ is consistent with all results using R-ratio.
- Recall that 2.5σ tension has existed for $\Delta\alpha^{(5)}_{\rm had}(-5GeV^2)$. The tension has diminished due to the error from higher energy.

QED Coupling at Z-pole Comparison II

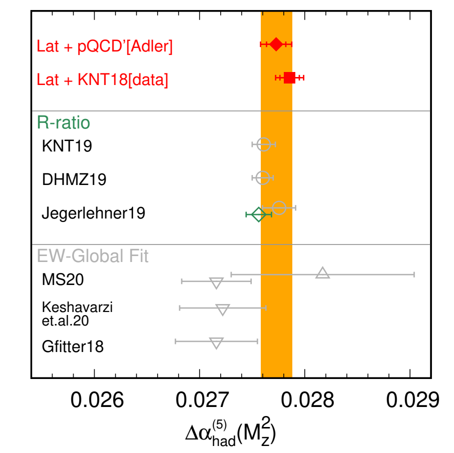

Figure: 5-flavor quark/hadron contributions to QED coupling at Z-pole.

Mainz LQCD, JHEP-2022

- First symbol ♦ is consistent with one of the Jehgerlehner's estimate ◊, which also adopted the Euclidean split method.
- The small difference solely results from the low energy contributions $\Delta\alpha^{(5)}_{\rm had}(-Q_0^2)$, where we used Mainz LQCD data while Jegerlehner did R-ratio data.

QED Coupling at Z-pole Comparison III

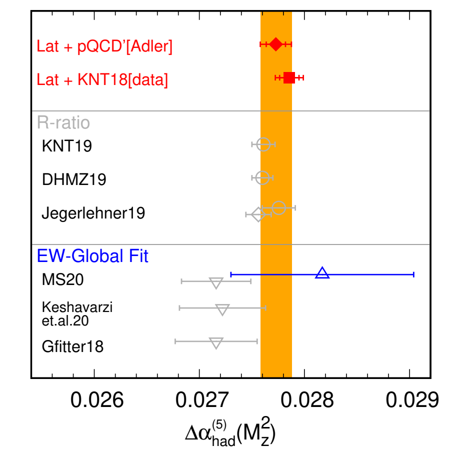

Figure: 5-flavor quark/hadron contributions to QED coupling at Z-pole.

Mainz LQCD, JHEP-2022

First symbol ♦ is consistent with one of the Malaescu-Schott's estimate △, which is from EW-Global fits with M_{higgs} left as a fit parameter (no-prior).

QED Coupling at Z-pole Comparison IV

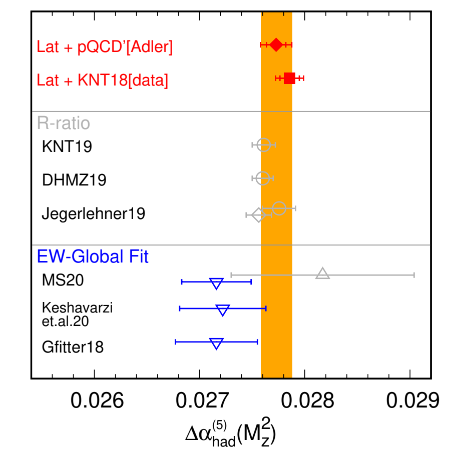

Figure: 5-flavor quark/hadron contributions to QED coupling at Z-pole.

Mainz LQCD, JHEP-2022

If $M_{higgs} = 125\ GeV$ is used as a prior, EW-Global fits gives $\triangledown$: As [Crivellin et al, PRL2020] pointed out, the SM Higgs favors somewhat lower $\Delta\alpha^{(5)}_{\rm had}(M_Z^2)$. However, the tension is at most 1.3σ. EW physics is not necessarily spoiled by the current LQCD HVP.

Table of Contents

Budapest-Marseille-Wuppertal Collaboration

**Sz. Borsanyi, Z. Fodor, J.N. Guenther, C. Hoelbling, S.D. Katz,
L. Lellouch, T. Lippert, K. Miura, L. Parato, K.K. Szabo, F. Stokes,
B.C. Toth, Cs. Torok, and L. Varnhorst.**

References

- arXiv:2002.12347. Published in Nature 2021.
- Phys. Rev. Lett. **121**, no. 2, 022002 (2018).
- Phys. Rev. D **96**, no. 7, 074507 (2017).

Reminder: How To Calculate $a_\mu^{\text{LO-HVP}}$

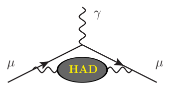

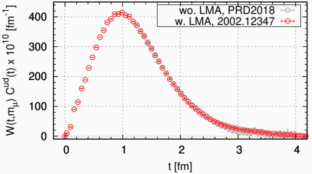

- **LQCD:**

$$a_\mu^{\text{LO-HVP}} = \sum_t W(t, m_\mu) G(t, D^{-1}[U]) \, .$$

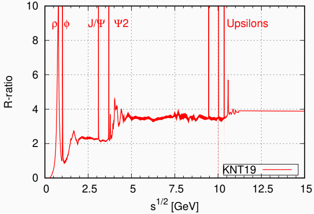

- **Data-Driven Pheno:**

$$a_\mu^{\text{LO-HVP}} = \int dQ^2 \, \omega(Q^2/m_\mu^2) \hat{\Pi}(-Q^2) \, ,$$

$$\hat{\Pi}(-Q^2) = \frac{Q^2}{12\pi^2} \int_0^\infty ds \, \frac{R(s)}{s(s+Q^2)} \, .$$

Long Distance Control

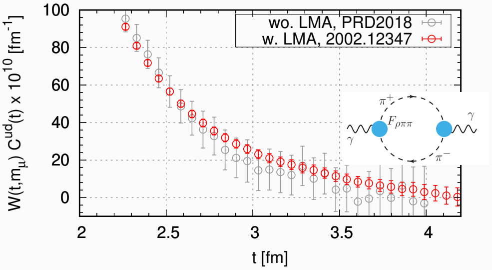

Fig: Zoom of long-distance region of the integrand of $a_{\mu,\,ud}^{\text{LO-HVP}} = (\frac{\alpha}{\pi})^2 \sum_t W(t, m_\mu^2) C^{ud}(t)$.

BMW-2020/2018 $a = 0.064\ fm$ e.g.

Need to control around $\hbar c/M_\pi \sim 4\ fm$.

Low-Mode Averaging (LMA)

- Get exactly Dirac eigen values/vectors $\{\lambda_n, v_n\}$ w. Lanczos-like method from below.
- Constract Dirac propagator as $D^{-1} = D_{\text{eig}}^{-1} + D_{\text{reft}}^{-1}$, where,

$$D_{\text{eig}}^{-1} = \sum_{\lambda_n \lesssim (m_s/2)} \frac{v_n v_n^\dagger}{\lambda_n}\ , \qquad D_{\text{rest}}^{-1} = D^{-1}\left(1 - \sum_{\lambda_n \lesssim (m_s/2)} v_n v_n^\dagger\right)\ . \tag{12}$$

The rest part D_{rest}^{-1} is stochastically evaluated (Conjugate Gradient).

WP2020 + BMW2020

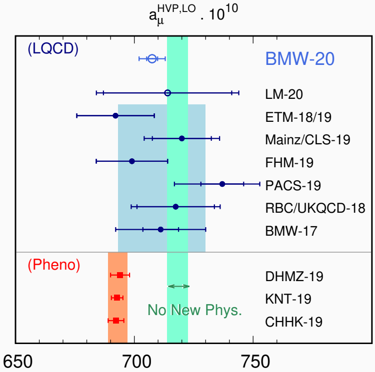

Figure: LO-HVP ($O(\alpha_0^2)$) muon g-2 comparison.

c.f. (No New Phys.)
= (FNAL/BNL) − (SM wo. LO-HVP).

WP2020(Phys.Rept. 887 (2020))

- $a_\mu^{\text{LO-HVP}} = 711.6(18.4) \cdot 10^{-10}$.
- Top-cited hep-ph paper of 2020!

BMW2020(Nature 593 (2021) 7857)

- $a_\mu^{\text{LO-HVP}} = 707.5(2.3)(5.0) \cdot 10^{-10},\ 0.8\%$
- Small Tension to “No New Physics”: LQCD-based *Interpretation* for FNAL/BNL.
- $(2.0/2.5/2.4)\sigma$ tension to DHMZ19/KNT19/CHHKS19.

The Window Analyses

Integrand of $a_{\mu,ud}^{\text{LO-HVP}}$

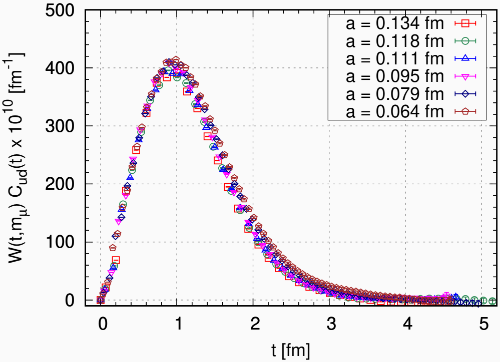

$$a_\mu^{\text{LO-HVP}} = \sum_t W(t, m_\mu) C^{lat}(t) \;, \tag{13}$$

$$c.f.\; C^{pheno}(t) = \int_0^\infty ds \sqrt{s} R_{had}(s) e^{-\sqrt{s}|t|} \;. \tag{14}$$

Integrand of $a_{\mu,ud}^{\text{LO-HVP}}$

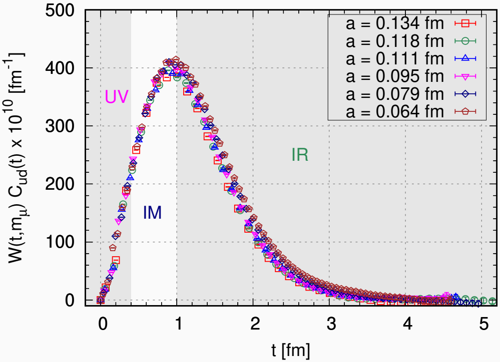

$$a_\mu^{\text{LO-HVP}} = \sum_t W(t, m_\mu) C^{lat}(t) \, , \tag{15}$$

$$c.f. \; C^{pheno}(t) = \int_0^\infty ds \sqrt{s} R_{had}(s) e^{-\sqrt{s}|t|} \, . \tag{16}$$

Window IR Threshold

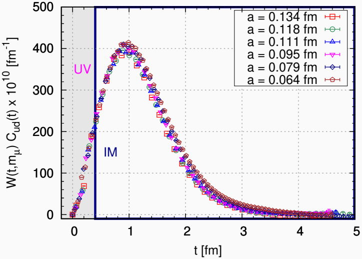

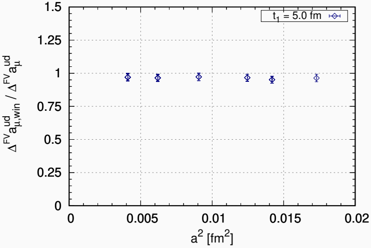

- FV: Spatially n-th wrapping pions w. pion form factor. [M. Hansen & A. Pattella, PRL2019, arXiv:200403935.]
- $t_0 = 0.4 fm$ (fixed) , $t_1 = 5.0 fm$.

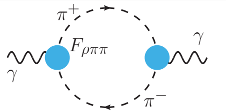

Window IR Threshold

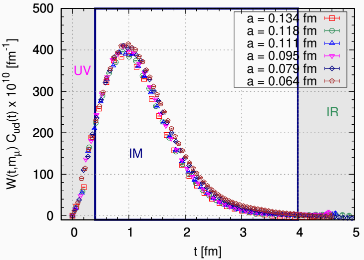

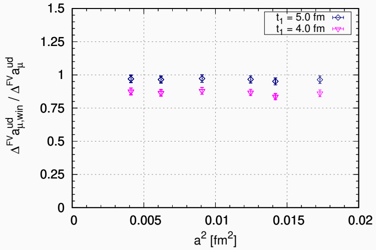

- FV: Spatially n-th wrapping pions w. pion form factor. [M. Hansen & A. Pattella, PRL2019, arXiv:200403935.]
- $t_0 = 0.4 fm$ (fixed) , $t_1 = 4.0 fm$.

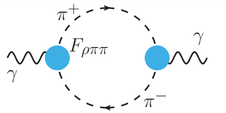

Window IR Threshold

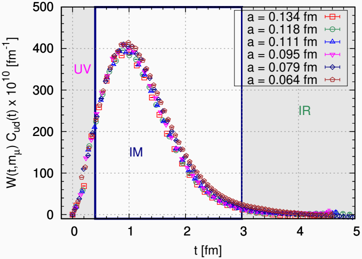

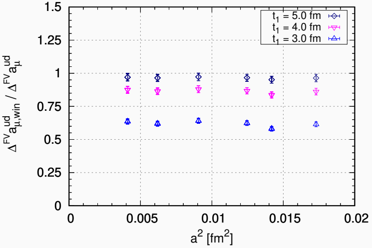

- FV: Spatially *n*-th wrapping pions w. pion form factor.
  [M. Hansen & A. Pattella, PRL2019, arXiv:200403935.]
- $t_0 = 0.4 fm$ (fixed) , $t_1 = 3.0 fm$.

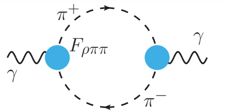

Window IR Threshold

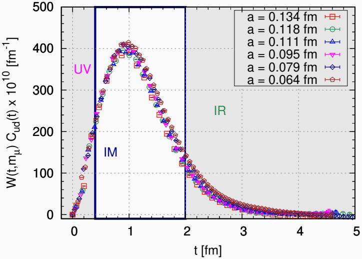

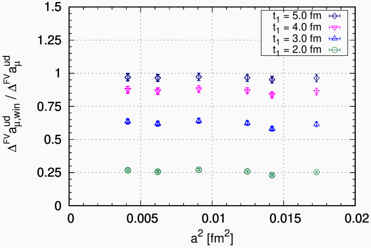

- FV: Spatially *n*-th wrapping pions w. pion form factor.
  [M. Hansen & A. Pattella, PRL2019, arXiv:200403935.]
- $t_0 = 0.4 fm$ (fixed) , $t_1 = 2.0 fm$.

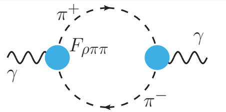

Window IR Threshold

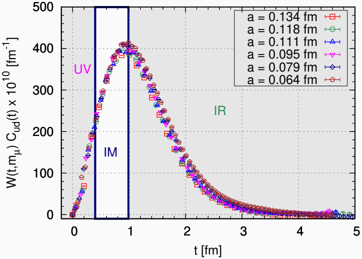

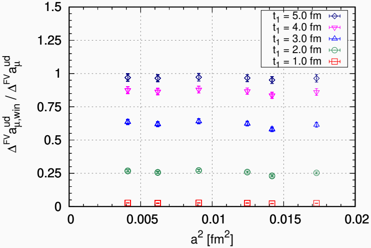

- FV: Spatially *n*-th wrapping pions w. pion form factor. [M. Hansen & A. Pattella, PRL2019, arXiv:200403935.]
- $t_0 = 0.4 fm$ (fixed) , $t_1 = 1.0 fm$.

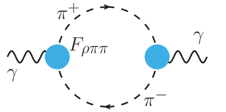

Window Method Comparison

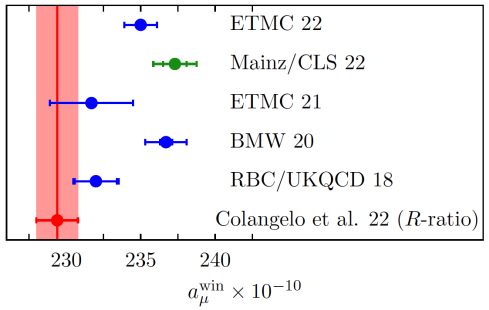

Fig: Thanks to Simon Kuberski. Update of arXiv:2206.06582.

- BMW-20: $a_\mu^{win} = 236.7(0.4)(1.3)[1.4] \cdot 10^{-10}$.
- Mainz/CLS-22: $a_\mu^{win} = 237.30(0.79)(1.22)[1.45] \cdot 10^{-10}$.
- The latest three LQCD: $0.5\% - 0.6\%$ precision, $3.5\sigma - 3.9\sigma$ tension to Data-Driven Pheno (R-ratio).

Table of Contents

Summary

- **Mainz/CLS: QED Coupling (JHEP-2022):**
  - $\Delta\alpha_{\text{had}}(-5\text{GeV}^2)$ is larger than Data-Driven Pheno w. 2.5σ tension.
  - $\Delta\alpha_{\text{had}}(M_Z^2) = 0.02773(15)$ is consistent with the Data-Driven Pheno and EW global fits.
- **BMW-Nature21:**
  - $a_\mu^{\text{LO-HVP}} = 707.5(2.3)(5.0) \cdot 10^{-10}$, 0.8% .
  - Small tension to No New Physics: $(718.2 \pm 4.4) \times 10^{-10}$.
  - $(2.0/2.5/2.4)\sigma$ tension to Data-Driven Pheno DHMZ19/KNT19/CHHKS19.
- **Window Analyses:**
  - BMW-20: $a_\mu^{win} = 236.7(0.4)(1.3)[1.4] \cdot 10^{-10}$.
  - Mainz/CLS-22: $a_\mu^{win} = 237.30(0.79)(1.22)[1.45] \cdot 10^{-10}$.
  - The latest LQCDs: $3.5\sigma - 3.9\sigma$ tension to Data-Driven Pheno (R-ratio).

Future Works

- Need to update LQCD $a_\mu^{\text{LO-HVP}}$ to per-mil presision consensus.
- Need to specify a source of LQCD-Pheno tensions:
  - Problem in modeling in $\sqrt{s} < 0.7 GeV$ in R-ratio? [Keshavarzi et.al.(2006.12666)].
  - Problem in modeling just after ϕ peak? [Mainz/CLS 2206.06582].